Crystal Interfaces and Microstructure

There are 3 types of interfaces;

− Free surfaces of a crystal (solid/vapour interface)

− Grain boundaries (α/α interfaces)

− Interphase interfaces (α/β interfaces)

α/β interphase interface plays an important role in determining the kinetics of phase transformations. The great majority of phase transformations occur by the growth of a new phase from a few nucleation sites within the parent phase. (nucleation and growth process)

The solid/vapour interface is important in vaporization and condensation transformation.

Grain boundaries are important in recrystallization, which is the transformation of a highly deformed grain structure into new undeformed grains.

Interfacial Free Energy

The free energy of a system containing an interface of area A and free energy γ per unit area is;

$$G = G_0 + A\gamma$$

G_0: free energy of the system assuming that all material has bulk property

γ: excess free energy arising because of the fact that some material lies close to interface.

Consider figure; Frame has a movable bar with a force F per unit length, must be applied to maintain the bar in position. If force moves a small distance, the film area increase dA, the work done by this motion is FdA.

The increase in free energy by this work is;

$$dG = \gamma dA + A d\gamma$$

equating with FdA; $\Rightarrow F = \gamma + A\dfrac{d\gamma}{dA}$
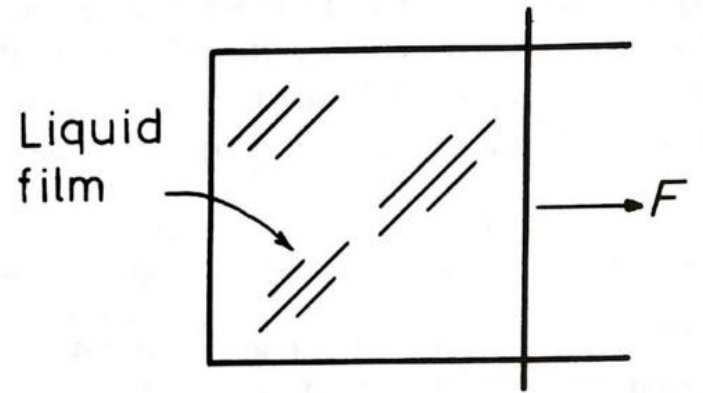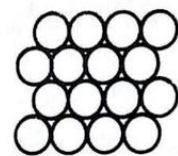

A liquid film on a wire frame.

In the case of a liquid film the surface energy is independent of the area of the interface, $d\gamma/dA = 0 \Rightarrow F = \gamma$ [the atoms in liq. can rearrange during stretching process and maintain a const. surface structure]
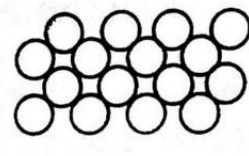
In solids, $d\gamma/dA \neq 0$, but at temperatures near the melting point the atomic mobility is usually high enough for $d\gamma/dA = 0$
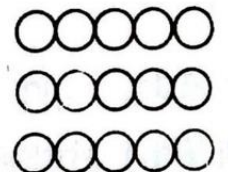
Solid/Vapor Interface

The origin of the surface free energy is that atoms in the layers nearest the surface are without some of their neighbours. On $\{111\}$ surface in the Figure, 3 of the 12 neighbours are missing on the surface. If bond strength is ε, $\varepsilon/2$ is lowered the internal energy of each atom.

111 200 220

For pure metal ε can be estimated from the heat of sublimation L_s.

If 1 mol of solid vaporized $12 N_a$ broken bonds are formed. Therefore $L_s = 12 N_a \, \varepsilon/2$.

Consequently the energy of a $\{111\}$ surface is $E_{sv} = 0.25 \, L_s/N_a$ J/surface atom.

This result is approximate since 2nd nearest neighbours have been ignored.

From the definition of Gibbs free energy, the surface free energy will be given by;

$$\gamma = E + PV - TS$$

'PV' term is ignored but surface entropy effects must be taken into account. Surface atoms will have more freedom of movement. Also extra configurational entropy can be introduced because of formation of surface vacancies.

Experimental measured values for pure metals indicate that near the melting temperature the surface free energy averaged over many surface planes is given by;

$$\gamma_{sv} = 0,15 \, L_s / N_a \quad J/\text{surface atom}$$

Some selected values of γ_{sv} at the melting point are listed below.
Note that metals with high melting temperatures have high L_s values and high γ_{sv}

When the macroscopic surface plane has a high or irrational $\{hkl\}$ index the surface will appear as a stepped layer structure where each layer is a close-packed plane (see Figure)

A crystal plane at on θ to the close-packed plane will contain broken bonds.
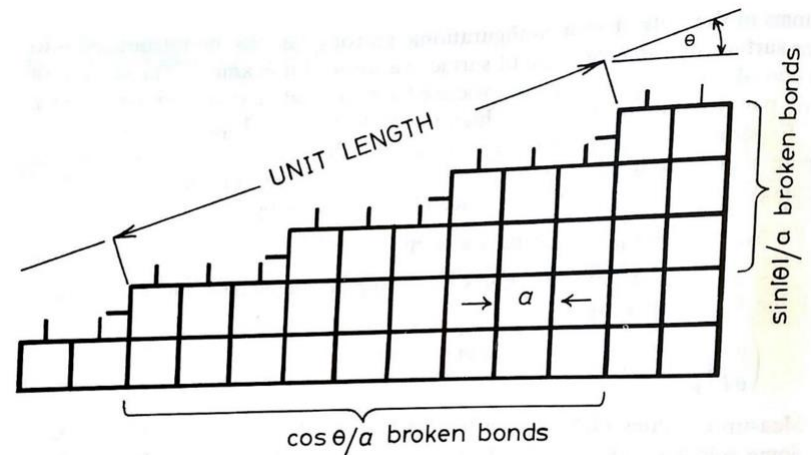
For unit length of interface; there will be

$(\cos\theta/a)(1/a)$ broken bonds and $(\sin|\theta|/a)(1/a)$ broken bonds from the atoms on the steps.

Again attributing $\varepsilon/2$ energy to each broken bond;

$$E_{sv} = (\cos\theta + \sin|\theta|)\,\frac{\varepsilon}{2a^2}$$

Crystal	$T_m/°C$	$\gamma_{sv}/mJ\ m^{-2}$
Sn	232	680
Al	660	1080
Ag	961	1120
Au	1063	1390
Cu	1084	1720
δ-Fe	1536	2080
Pt	1769	2280
W	3407	2650

The 'broken-bond' model for surface energy.

This is plotted as a function of θ in Figure. Note that the close-packed orientation ($\theta = 0$) lies at the minimum in the energy plot. Similar arguments can be applied to any crystal structure for rotations about any axis from any reasonably close-packed plane.

If γ is plotted vs. θ similar cusps (peak) are found. Low-index planes should be located at low-energy positions (wells).
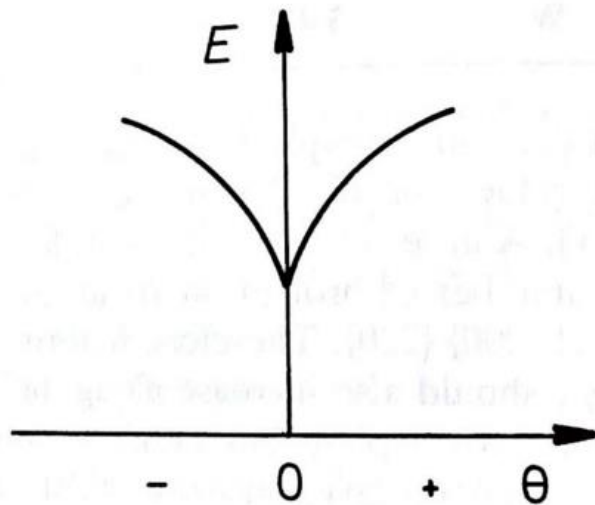

Variation of surface energy as a function of θ

A convenient method for plotting the variation of γ with surface orientation in 3-D is to construct a surface about an origin such that the <u>free energy</u> <u>of any plane is equal to the distance between the surface and the origin when</u> <u>measured along the normal to the plane in question.</u>

This type of polar representation of γ is known as γ-plot and has the useful property of being able to predict the equilibrium shape of an isolated single crystal.

(001)

A Wulff plane

γ plot

(111)

γ_{001}

B

A

γ_A

C

γ_{111}

O

(110)

Equilibrium shape
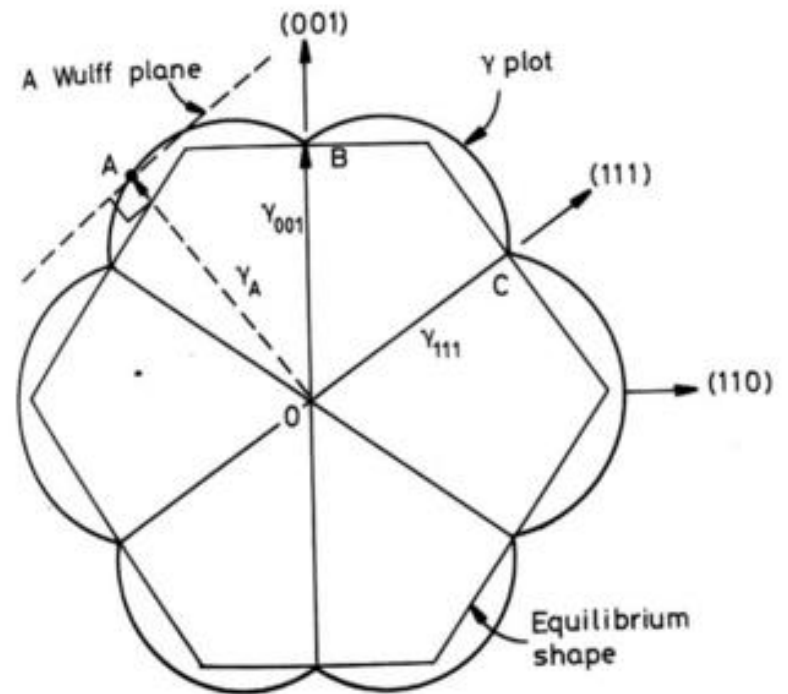
Diamond (FCC)
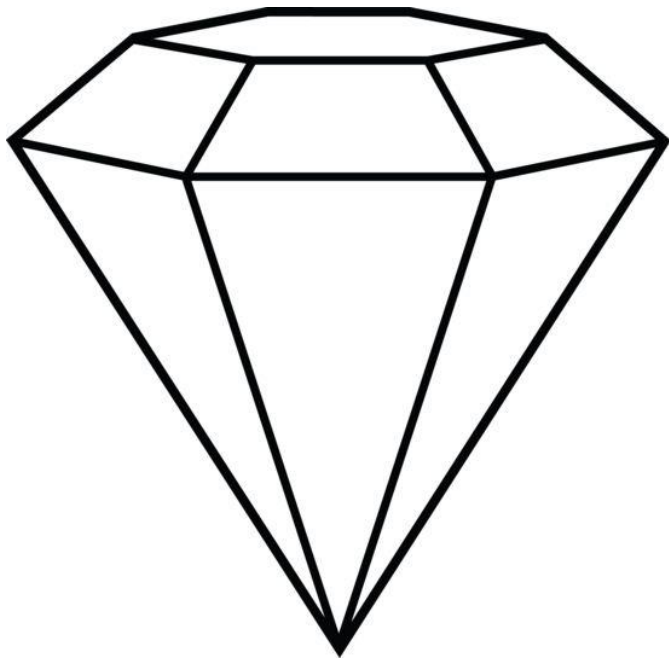
Boundaries in Single-Phase Solids

The grains in a single-phase polycrystalline specimen are generally in many different orientations and many different types of grain boundary. The nature of any given boundary depends on the misorientation of the two adjoining grains and the orientation of the boundary plane relative to them. The lattices of any two grains can be made to coincide by rotating one of them through a suitable angle about a *single* axis, giving pure tilt boundaries and pure twist boundaries, as illustrated in Figure (a) and (b).

A tilt boundary occurs when the axis of rotation is parallel to the plane of the boundary (a), whereas a twist boundary is formed when the rotation axis is perpendicular to the boundary (b).
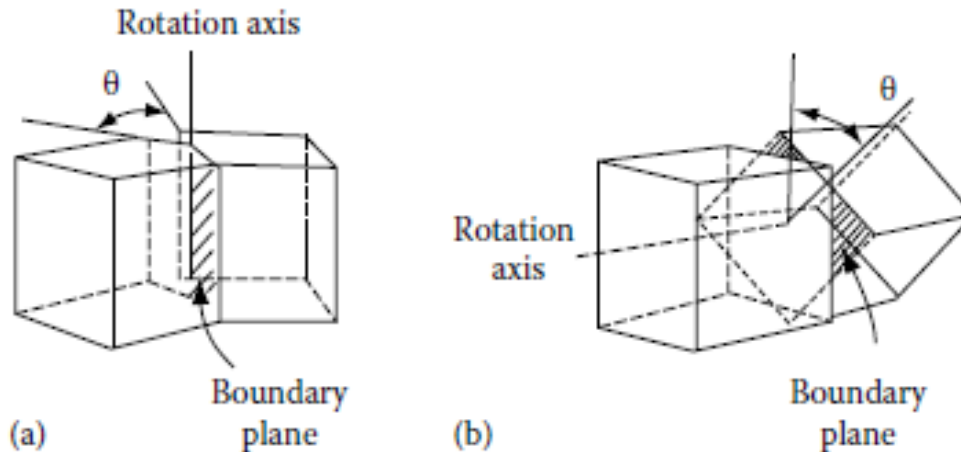
L ow-Angle and High-Angle Boundaries

These are symmetrical *low-angle tilt* and *low-angle twist* boundaries. The low angle tilt boundary is an array of parallel edge dislocations, whereas the twist boundary is a cross-grid of two sets of screw dislocations.
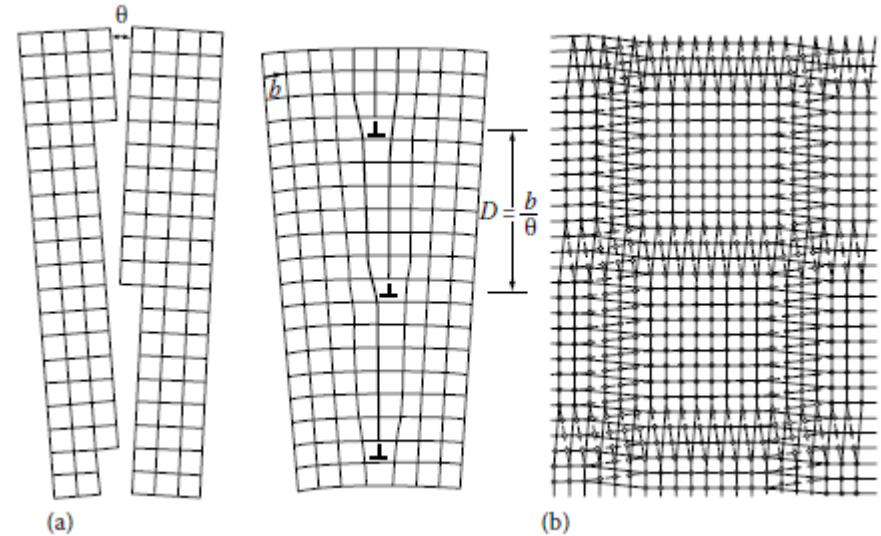
The energy of a low-angle grain boundary is simply the total energy of the dislocations within unit area of boundary. This depends on the spacing of the dislocations which, for the simple arrays in Figure, is given by

$$D = \frac{b}{\sin\theta} \approx \frac{b}{\theta}.$$

where *b* is the Burgers vector of the dislocations and θ is the angular misorientation across the boundary.
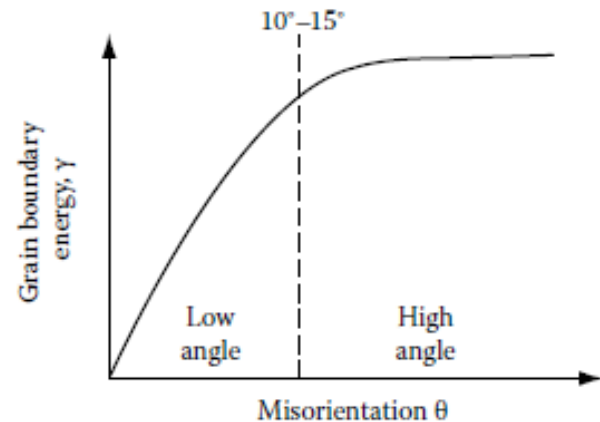
At very small values of θ the dislocation spacing is very large and the grain boundary energy γ is approximately proportional to the density of dislocations in the boundary $(1/D)$, i.e.

$$\gamma \propto \theta$$

However as θ increases the strain fields of the dislocations progressively cancel out so that γ increases at a decreasing rate as shown in previous Figure.

In general when θ exceeds 10-15^0 the dislocation spacing is so small that the dislocation cores overlap and it is then impossible to physically identify the individual dislocations. At this stage the grain-boundary energy is almost independent of misorientation (see previous figure)

Grain-boundary transition zone
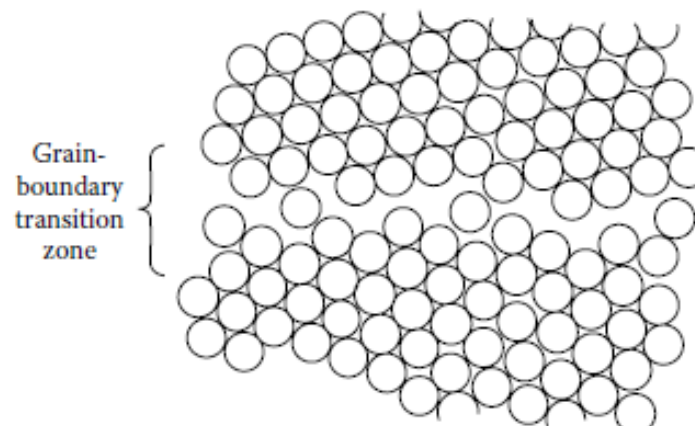
When $\theta > 10$–15^0 the boundary is known as a *random high-angle grain boundary*. The difference in structure between low-angle and high-angle grain boundaries is lucidly illustrated by the bubble-raft model in Figure below
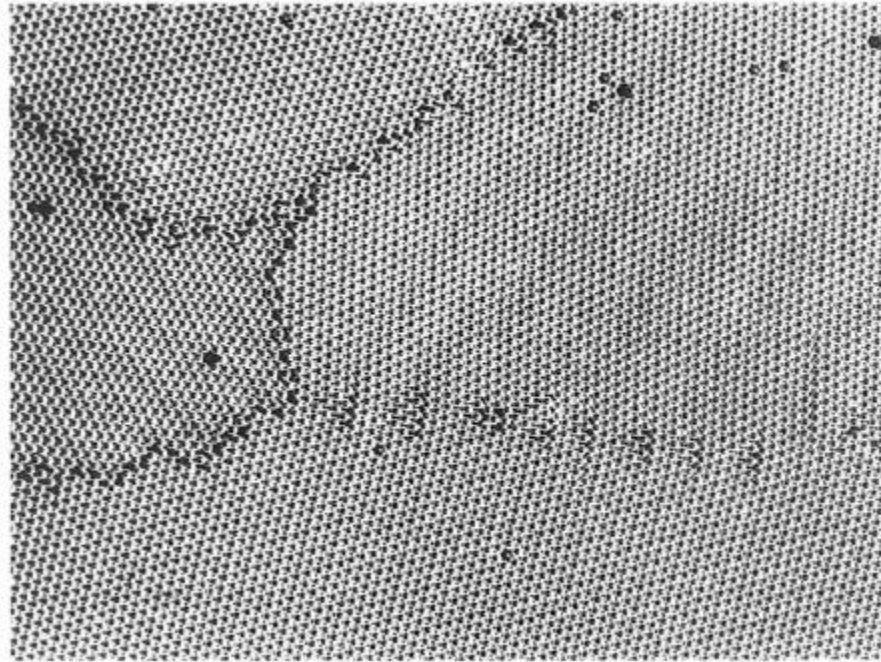
High angle boundaries contain large areas of poor fit and have a relatively open structure. The bonds between the atoms are broken or highly distorted and consequently the boundary is associated with a relatively high energy.

Measured high-angle grain boundary energies γ_b are often found to be roughly given by

$$\gamma_b \simeq \frac{1}{3}\gamma_{sv}$$

Some selected values for γb and γ_b/γ_{sv} are listed in Table

Measured Grain Boundary Free Energies

Crystal	γ_b/mJ m^{-2}	T/°C	γ_b/γ_{sv}
Sn	164	223	0.24
Al	324	450	0.30
Ag	375	950	0.33
Au	378	1000	0.27
Cu	625	925	0.36
7-Fe	756	1350	0.40
γ-Fe	468	1450	0.23
δt	660	1300	0.29
W	1080	2000	0.41

Source: Values selected from compilation given in *Interfacial Phenomena in Metals and Alloys*, by L.E. Murr, Addison-Wesley, London, 1975.

Special High-Angle Grain Boundaries

Not all high-angle boundaries have an open disordered structure. There are some *special high-angle boundaries* which have significantly lower energies than the random boundaries. These boundaries only occur at particular misorientations and boundary planes which allow the two adjoining lattices to fit together with relatively little distortion of the interatomic bonds.

The simplest special high-angle grain boundary is the boundary between two twins. If the twin boundary is parallel to the twinning plane the atoms in the boundary fit perfectly into both grains. The result is a *coherent twin boundary* as illustrated in Fig

(a)   (b)
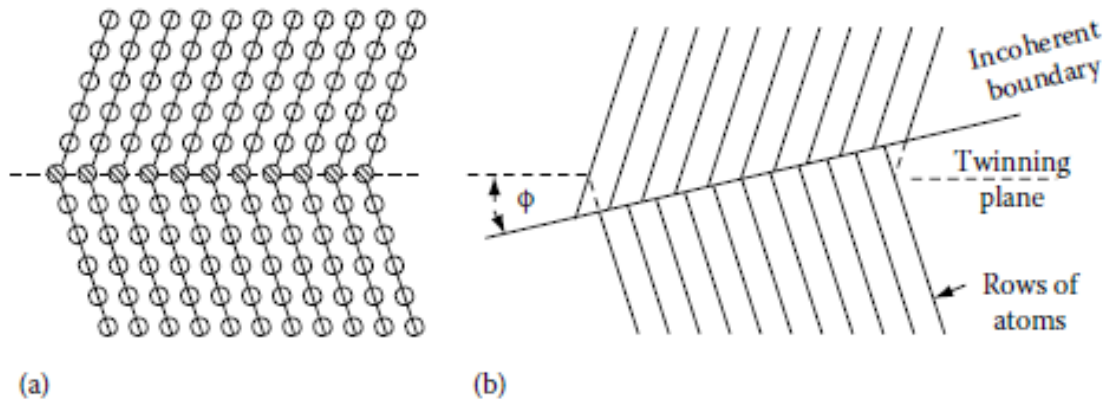
If the twin boundary does not lie exactly parallel to the twinning plane, Figure, the atoms do not fit perfectly into each grain and the boundary energy is much higher. This is known as an *incoherent twin boundary*.

The energy of a twin boundary is therefore very sensitive to the orientation of the boundary plane. If γ is plotted as a function of the boundary orientation a sharp cusped minimum is obtained at the coherent boundary position as shown in Figure
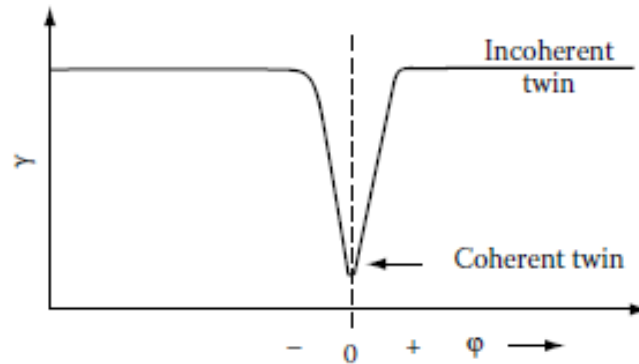

Table lists some experimentally measured values of coherent and incoherent twins along with high-angle grain boundary energies for comparison

Measured Boundary Free Energies for Crystals in Twin Relationships (Units mj m^{-2})

Crystal	Coherent Twin Boundary Energy	Incoherent Twin Boundary Energy	Grain Boundary Energy
Cu	21	498	623
Ag	8	126	377
Fe-Cr-Ni (stainless steel type 304)	19	209	835

Source: Values selected from compilation given in *Interfacial Phenomena in Metals and Alloys*, by L.E. Murr, Addison-Wesley, London, 1975.

Equilibrium in Poly Crystalline Materials

Different grain-boundary energies affects the microstructure of a polycrystalline material. Figure shows the microstructure of an annealed austenitic stainless steel (fcc). The material contains high- and low-angle grain boundaries as well as coherent and incoherent twin boundaries.
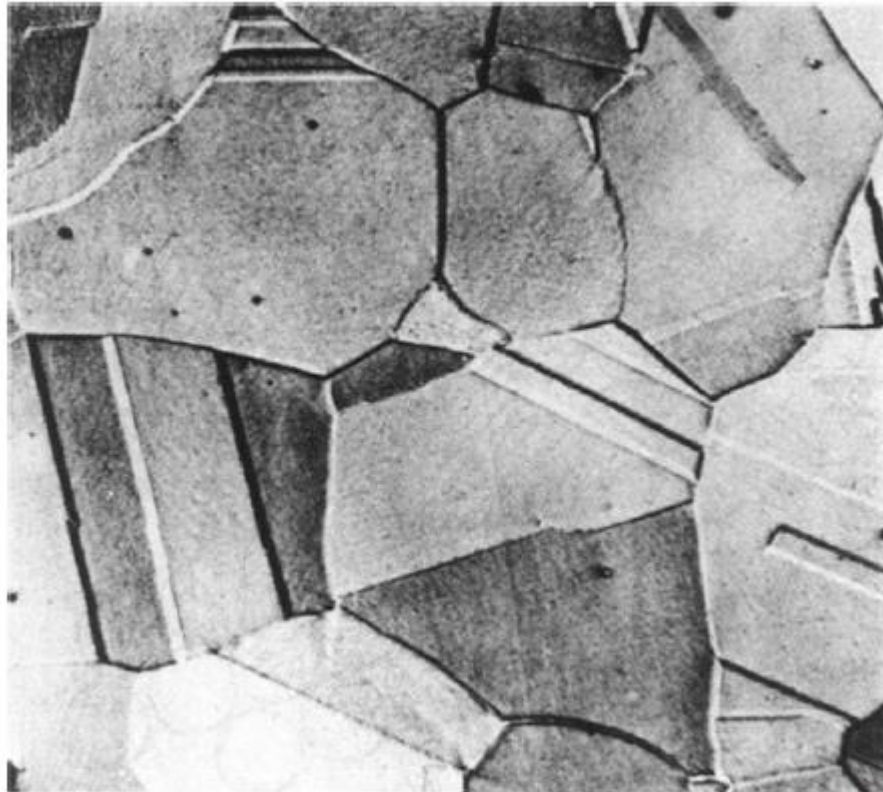
Microstructure of an annealed crystal of austenitic stainless steel. (After P.G. Shewmon, *Transformations in Metals*, McGraw-Hill, New York, 1969.)

This microstructure is determined by how the different grain boundaries join together in space. When looking at two dimensional microstructures like this it is important to remember that in reality the grains fill three dimensions, and only one section of the three dimensional network of internal boundaries is apparent.

Note that two grains meet in a plane (a grain boundary), three grains meet in a line (a grain edge) and four grains meet at a point (a grain corner). Let us now consider the factors that control the grain shapes in a recrystallized polycrystal.

The first problem to be solved is why grain boundaries exist at all in annealed materials. The boundaries are all high-energy regions that increase the free energy of a polycrystal relative to a single crystal. Therefore a polycrystalline material is never a true equilibrium structure. However the grain boundaries in a polycrystal can adjust themselves during annealing to produce a *metastable* equilibrium at the grain boundary intersections

The conditions for equilibrium at a grain-boundary junction can be obtained either by considering the total grain boundary energy associated with a particular configuration or, more simply, by considering the forces that each boundary exerts on the junction.

First consider a grain-boundary segment of unit width and length OP as shown in Fig
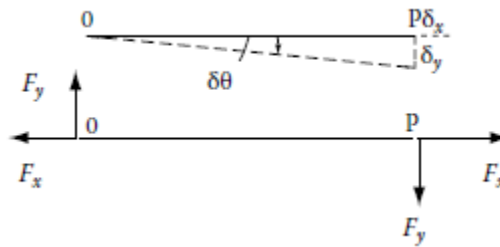
If the boundary is mobile then forces F_x and F_y must act at O and P to maintain the boundary in equilibrium.

Remember $(F=\gamma)$, then $F_x = \gamma$. F_y can be calculated as follows: if P is moved a small distance δy while O remains stationary, the work done will be $F_y \delta_y$. This must balance the increase in boundary energy caused by the change in orientation $\delta\theta$, i.e.

$$F_y \delta_y = l \frac{d\gamma}{d\theta} \delta\theta$$

Since $\delta_y = l\delta\theta$ $F_y = \dfrac{d\gamma}{d\theta}$
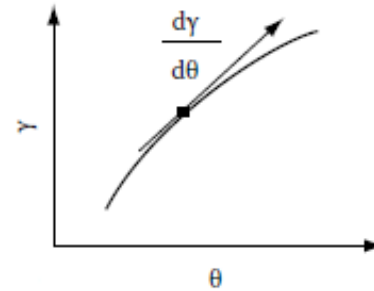
This means that if the grain-boundary energy is dependent on the orientation of the boundary a force $d\gamma/d\theta$ must be applied to the ends of the boundary to prevent it rotating into a lower energy orientation.

$d\gamma/d\theta$ is therefore known as a *torque term*. Since the segment OP must be supported by forces *Fx* and *Fy* the boundary exerts equal but opposite forces *–Fx* and *–Fy* on the ends of the segment which can be junctions with other grain boundaries.

If the boundary energy is independent of orientation the torque term is zero and the grain boundary behaves like a soap film. Under these conditions the requirement for metastable equilibrium at a junction between three grains, Figure, is that the boundary tensions $\gamma1$, $\gamma2$ and $\gamma3$ must balance. In mathematical terms

$$\frac{\gamma_{23}}{\sin \theta_1} + \frac{\gamma_{13}}{\sin \theta_2} = \frac{\gamma_{12}}{\sin \theta_3}$$
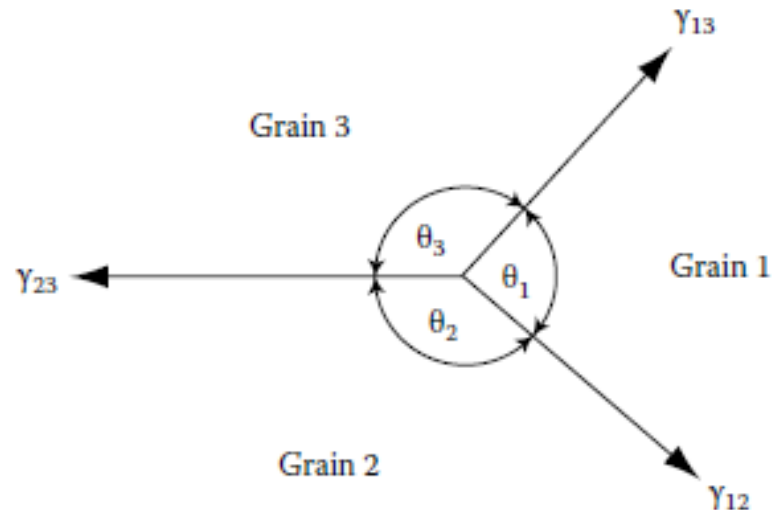
One method of measuring grain-boundary energy is to anneal a specimen at a high temperature and then measure the angle at the intersection of the surface with the boundary (figure). If the solid-vapour energy (γ_{sv}) is the same for both grains, balancing the interfacial tensions gives

$$2\gamma_{sv}\cos\frac{\theta}{2} = \gamma_b$$
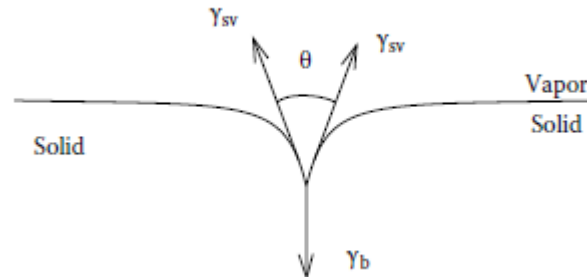
Exercise

Please draw the free energy-composition curves for the system in figure for all temperatures